Available online at www.sciencedirect.com
ScienceDirect
Catalysis Today 127 (2007) 330–336
CATALYSIS TODAY
www.elsevier.com/locate/cattod

Study of the water gas shift reaction on Fe in a high temperature proton conducting cell

Christos Kokkofitis, George Karagiannakis, Michael Stoukides *

Chemical Engineering Department, Aristotle University & Chem. Proc. Engineering Research Institute, U. Box 1517, University Campus, Thessaloniki 54124, Greece

Available online 19 June 2007

Abstract

The water gas shift (WGS) reaction was studied in a double-chamber high temperature proton conducting cell (HTPC). The proton conductor was a strontia–ceria–ytterbia (SCY) disk of the form: $SrCe_{0.95}Yb_{0.05}O_{3-\alpha}$ and the working electrode was a polycrystalline Fe film. The reaction temperature and the inlet partial pressure of CO varied between 823 and 973 K, and between 1.0 and 10.6 kPa, respectively. The inlet partial pressure of steam (P_{H_2O}) was kept constant at 2.3 kPa. An increase in the production of H_2 was observed upon ''pumping'' protons away from the catalyst surface. The Faradaic efficiency (Λ) was lower than unity, indicating a sub-Faradaic effect. The highest value of rate enhancement ratio (ρ) was approximately 3.2, at $T = 823$ K. The proton transport number (PTN) varied between 0.45 and 1.0. An up to 99% of the produced H_2 was electrochemically separated from the reaction mixture.

Keywords: High temperature proton conductor; Water gas shift reaction; H_2 production; Electrocatalytic separation of H_2; Fe catalyst

1. Introduction

With hydrogen appearing as the energy ''currency'' of the future, there is an ongoing interest in technologies associated with hydrogen production and purification. The water gas shift (WGS) reaction is a well-established process that mostly applies to large scale steady-state operations, such as hydrogen or ammonia plants [1–3]. It is an exothermic reaction and therefore thermodynamically favored at low temperatures:

$$CO + H_2O \rightarrow CO_2 + H_2 \quad \Delta H^\circ = -41.1\,\text{kJ/mol} \quad (\text{at } 298\,\text{K}). \tag{1}$$

Recently, the need for the development of efficient fuel processors in fuel cell applications has strongly renewed the interest for the above reaction. To this end, a large number of investigators have studied the WGS reaction over a variety of metal or metal oxide catalysts; either supported on oxide supports [1–9] or unsupported [10–15]. Although current research efforts mostly focus on noble metal-based catalysts [1–8], the interest for Fe-based catalysts is still active [14–17].

Additionally, in an effort to achieve higher H_2 yields, several research groups have studied the WGS reaction in membrane reactors [18–20]. These reactors utilized primarily Pd or Pd–Ag membranes and their operation was based on the chemical potential difference of hydrogen between the two sides of the membrane. Another alternative is a proton conducting cell-reactor. The discovery of solid state materials that exhibit protonic (H^+) conductivity at elevated temperatures made it possible to use them in catalytic hydro- and dehydrogenations of industrial interest [21,22]. The prominent advantage of such an electrochemical reactor is that it offers simultaneous production and separation of hydrogen; the catalytic reaction takes place at the anode, while high purity H_2 is recovered at the cathode.

Proton conducting cell-reactors can be also used to electrochemically promote catalytic reaction rates. If the catalyst to be promoted is one of the electrodes of the cell, protons can be electrochemically ''pumped'' to or away from the catalyst during reaction. This can cause a considerable change in catalytic activity and the rate enhancement can be orders of magnitude higher than the rate of proton transport through the electrolyte [23,24].

* Corresponding author. Tel.: +30 2310 996165; fax: +30 2310 996145.
E-mail address: stoukidi@cperi.certh.gr (M. Stoukides).

0920-5861/$ – see front matter © 2007 Elsevier B.V. All rights reserved.
doi:10.1016/j.cattod.2007.05.007

In the present work, the WGS reaction is studied on a Fe catalyst-electrode in a double-chamber proton conducting cell-reactor. The reaction is studied under both, open and closed circuit and the effect of imposed current on the rates of formation and extraction of hydrogen is evaluated. The present results are compared to those obtained on Pd, conducted in a similar cell-reactor [25].

2. Experimental

A detailed description of the experimental apparatus and of the cell-reactor can be found in previous communications [26,27]. A schematic diagram of the double-chamber cell-reactor is shown in Fig. 1. The H^+ conductor was a strontia–ceria–ytterbia (SCY) disk of the form: $SrCe_{0.95}Yb_{0.05}O_{3-\alpha}$. The disk was prepared according to the recipe proposed by Iwahara et al. [28] and its thickness was about 1.5 mm.

The anode (catalyst) was a porous Fe film prepared from a Fe paste (Engelhard OL56C) and deposited on the inside surface of the SCY disk (Fig. 1). Similarly, the cathode was prepared from a Ag paste (Alfa Aesar #41823) and was deposited on the outside surface of the SCY disk. The two electrodes were calcined in air for 1 h at 1073 K. The catalyst (Fe) loading was 25 mg. SEM photographs (Fig. 2) showed that the Fe crystallites had an average particle size of 1 μm. Using this crystallite size, a catalytic surface area of 190 cm^2 was calculated. The superficial surface areas of the working (anodic) and counter (cathodic) electrode were 1.5 and 3 cm^2, respectively. Gold wires (0.4 mm diameter) were used to connect the two electrodes to the galvanostat.

Reactant gases and diluents were of 99.999% purity. The inlet (CO, H_2O, He) and outlet (CO, H_2O, CO_2, H_2, He) gaseous streams were analyzed on line by using a Shimadzu GC-14B

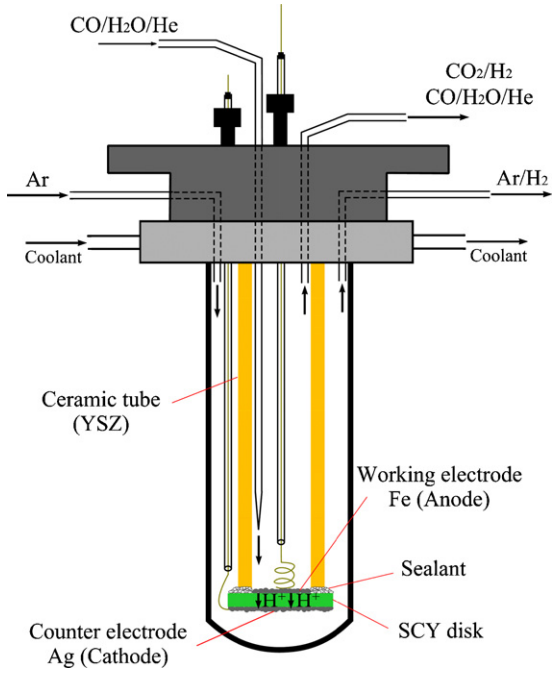

Fig. 1. Schematic diagram of the double-chamber cell-reactor.

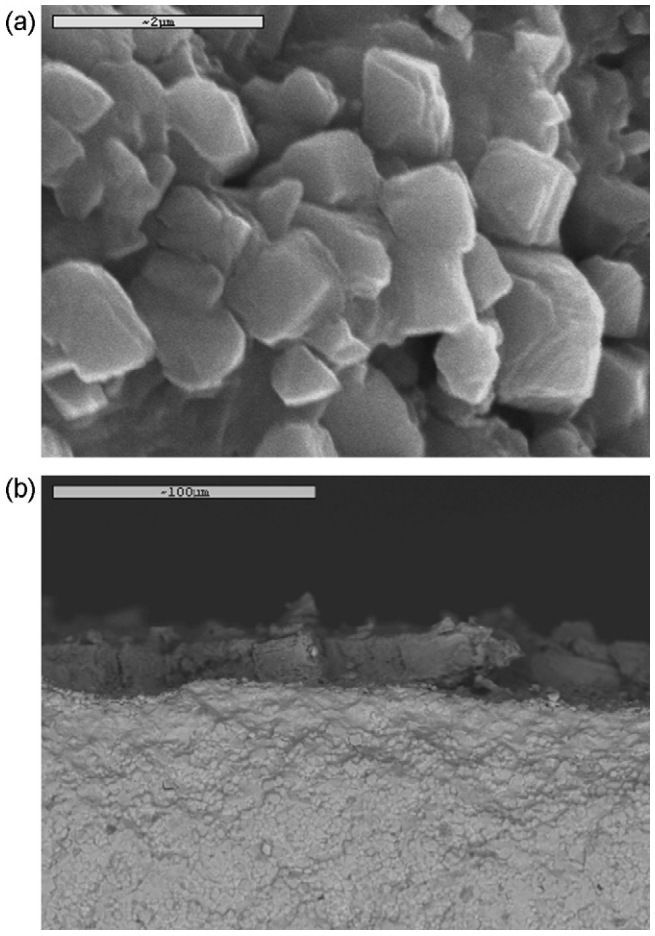

Fig. 2. Scanning electron micrographs for used Fe catalyst-electrode exposed to reaction conditions for a period of five weeks: (a) at ×20,000 magnification and (b) at ×500 magnification.

gas chromatograph with a thermal conductivity detector. A Porapak QS column was used to separate CO_2 and H_2O, while a Molecular Sieve 13× was used to separate CO and H_2. Additionally, the concentrations of CO and CO_2 were continuously monitored by means of a Binos infrared CO and CO_2 analyzer. Constant currents and voltages across the cell were imposed using a 2053 AMEL Galvanostat-Potentiostat.

The reaction mixture was prepared by bubbling a CO–He stream through a vessel that contained liquid water, at ambient temperature. The CO/H_2O/He mixture was then introduced over the anode (inner chamber) where hydrogen was produced by the WGS reaction. By imposing an electrical current through the cell, hydrogen was electrochemically transported from the anode to the cathode (outer chamber) in the form of H^+. At the cathode, protons were discharged and combined to produce gaseous H_2.

Under open-circuit (i.e. with no current passing through the solid electrolyte), the cell-reactor operates as a regular catalytic reactor. Reactants are co-fed over the anode which also serves as the catalyst for the WGS reaction. Under closed circuit, the cell-reactor operates as electrochemical hydrogen "pump". Using an external power source, a current (I) can be imposed through the electrolyte. Vayenas et al. [23,24] have defined the

Faradaic efficiency (Λ) as:

$$\Lambda = \frac{\Delta r}{I/2F} \tag{2}$$

where Δr is the change in the rate of hydrogen consumption or production and $I/2F$ is the imposed flux of H^+ (expressed in moles of H_2/s) through the electrolyte. If $\Lambda = 1$, the effect is Faradaic. In many studies reported thus far, Λ values exceeding unity by several orders of magnitude have been observed. This phenomenon is called NEMCA, i.e. non-Faradaic electrochemical modification of catalytic activity.

If the solid electrolyte shows pure protonic conductivity, Eq. (2) is valid as is. If not, Eq. (2) has to be modified to include the proton transport number (PTN):

$$\text{PTN} = \frac{\text{moles of } H_2 \text{ transferred through the proton conductor per second}}{I/2F} \tag{3}$$

Eq. (3) shows that PTN is the fraction of the total current that is carried through the solid electrolyte in the form of H^+. In the present study, PTN was experimentally determined by measuring the current I and the hydrogen flux through the SCY disk. Hence, Eq. (2) is now modified as:

$$\Lambda = \frac{\Delta r}{(I/2F)\text{PTN}} \tag{4}$$

In addition to the Λ factor, Vayenas et al. [23,24] defined another useful dimensionless parameter, the rate enhancement ratio, ρ:

$$\rho = \frac{r}{r_o} \tag{5}$$

where r is the reaction rate obtained under electrocatalytic mode of operation and r_o is the open-circuit catalytic rate (i.e. at $I = 0$).

The catalytic and electrocatalytic measurements were obtained at 823–973 K and at atmospheric total pressure. The partial pressure of H_2O (P_{H_2O}) was kept at 2.3 kPa, while the partial pressure of CO (P_{CO}) varied from 1 to 10.6 kPa. The reactants were fed to the inner chamber at a total volumetric flow rate of 100 cm^3/min. A stream of 20 cm^3/min of pure Ar was introduced over the cathodic electrode. This was done in order to obtain an accurate (gas chromatograph) measurement of H_2 transported from the inner to the outer chamber. This, in turn, was used to calculate PTN from Eq. (3). The catalytic results were obtained after approximately 24 h on stream. At all temperatures and reactant compositions examined, the only reaction products detected were CO_2 and H_2. It must be noted that, in all cases, the polarity of the imposed current/potential was in the direction of pumping protons from the catalyst (anode) to the cathode.

3. Results and discussion

First, the gas-phase (non-catalytic) WGS reaction was studied in order to determine its contribution to the overall reaction rate. It was found that the non-catalytic reaction rates were about 2–5% of the total reaction rate at the highest temperature examined (973 K). The results presented have been corrected by subtracting the non-catalytic contribution. The conversion of steam varied from 0.4% to 9% while that of CO was even lower; it varied from 0.4% to 7%. Actually, in 90% of the data points the conversions of either reactant were less than 5%. Therefore, differential conditions can apply.

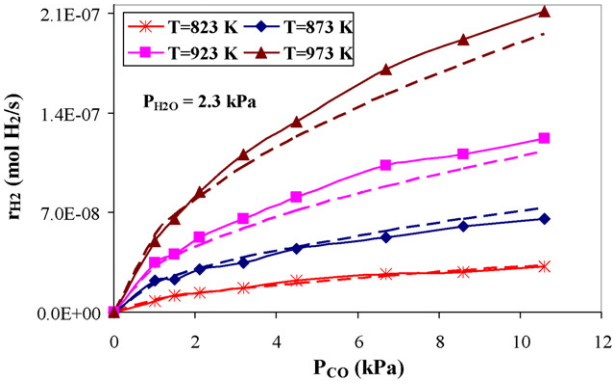

Fig. 3. Dependence of WGS reaction rate on P_{CO} at various reaction temperatures, under open-circuit operation. P_{H_2O} = 2.3 kPa.

Fig. 3 shows the dependence of the open-circuit reaction rate (r_o) on P_{CO} at constant P_{H_2O} (2.3 kPa). The continuous lines are curves passing from the catalytic data and the dotted lines are simulation curves generated by the kinetic model presented below. It can be seen that at low P_{CO} values, there is an almost linear increase in the reaction rate but at higher P_{CO} values, the dependence on P_{CO} weakens and the reaction rate gradually levels off. The reaction rates obtained here are 4–5 times lower than those observed on Pd electrodes, in a similar solid electrolyte cell [25]. This is in agreement with previous studies of the WGS reaction in which the catalytic activities of Fe and Pd were compared [16,29].

The two dominant mechanisms proposed for the WGS reaction are the redox mechanism and the formate-intermediate mechanism [1–17]. Most of the researchers agree that on Fe-based catalysts, the reaction proceeds via the formate-intermediate path [4,9,15,17]. Hence, that mechanism was assumed to interpret the present results: adsorbed CO reacts with hydroxyl (OH) groups, formed by dissociation of H_2O, to produce formate (HCOO) species, which consequently decompose to form CO_2 and H_2. The latter step (formate decomposition) is considered to be the rate-determining step (rds) of the reaction [15,17]. Based on these assumptions and for low reaction conversions (low P_{CO_2} and P_{H_2}), the simplified kinetic equation becomes:

$$r = k_I P_{CO}^a P_{H_2O}^b \tag{6}$$

where k_I is the reaction constant and 'a' and 'b' indicate the apparent reaction order with respect to CO and H_2O, respectively.

In the present experiments, the partial pressure of water, P_{H_2O}, was kept constant at 2.3 kPa. Therefore, for $k = k_I P_{H_2O}^b$,

the kinetic model can be further simplified to the following expression:

$$r = kP_{CO}^{a} \quad (7)$$

By simulating the experimental (catalytic) data with the above kinetic model, the values of the parameters were found to be:

$$a = 0.51 \pm 0.04 \quad (8)$$

$$k = 7.91 \times 10^{-4} \exp\left(\frac{-9309}{T}\right) \quad (9)$$

According to Eq. (9), the activation energy for the catalytic reaction is approximately 77.4 kJ/mol. This value is in very good agreement with previous studies of the WGS over Fe-based catalysts. Grenoble et al. [4] reported an apparent activation energy of 80.3 ± 5.4 kJ/mol for a Fe-Al_2O_3 catalyst while Rethwisch and Dumesic [9], who studied the reaction at elevated temperatures (620–720 K) over supported iron oxide reported an activation energy between 80 and 86 kJ/mol. Additionally, Teng et al. [15], who studied the reaction over Fe–Mn catalysts, calculated an activation energy of approximately 82 kJ/mol. The dotted curves shown in Fig. 3 have been obtained by applying the parameters as calculated by Eqs. (8) and (9) to the proposed kinetic model. It can be seen that there is a very good agreement between experimental results and model predictions.

Fig. 4 contains closed-circuit potentiometric results. A constant cell potential $E_{cell} = +2.5$ V is imposed and thus, protons (H^+) were "pumped" from the anode (Fe) to the cathode (Ag). The dependence of the reaction rate on P_{CO} is shown at various temperatures between 823 and 973 K. A comparison of the data of Fig. 4 to those of Fig. 3 indicates that H^+ pumping causes an increase in the reaction rate. Using Eq. (7) and the data of Fig. 4, new values for "a" and "k" were calculated, i.e.:

$$a' = 0.36 \pm 0.15, \quad (10)$$

$$k' = 9.24 \times 10^{-6} \exp\left(\frac{-4740}{T}\right) \quad (11)$$

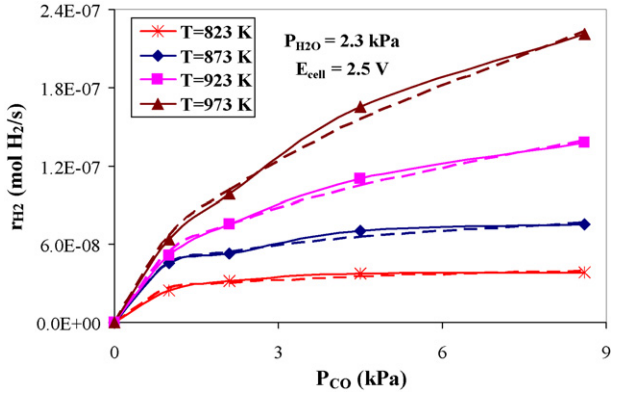

Fig. 4. Dependence of WGS reaction rate on P_{CO} at various reaction temperatures, under closed-circuit operation. $E_{cell} = 2.5$ V, $P_{H_2O} = 2.3$ kPa.

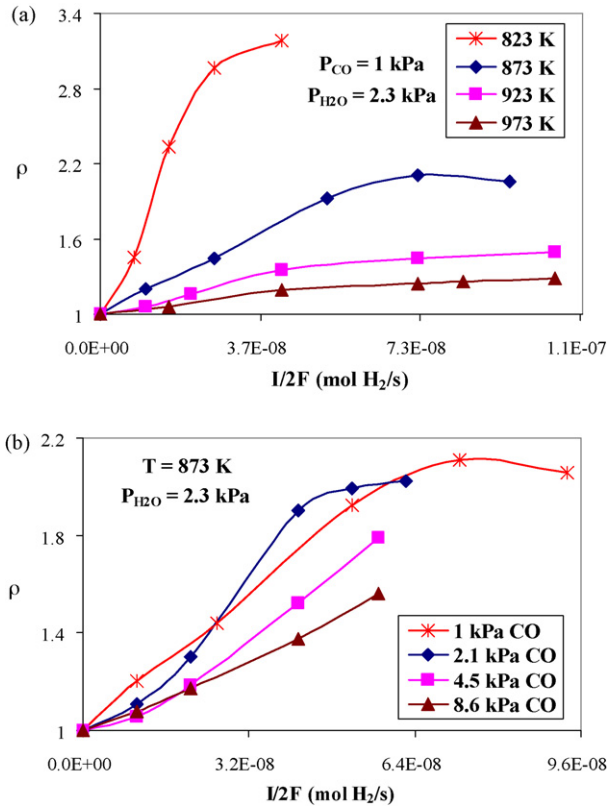

Fig. 5. (a) Dependence of rate enhancement ratio (ρ) on I/2F at various reaction temperatures. $P_{CO} = 1$ kPa, $P_{H_2O} = 2.3$ kPa. (b) Dependence of rate enhancement ratio (ρ) on I/2F for various P_{CO}. $T = 873$ K, $P_{H_2O} = 2.3$ kPa.

from which an activation energy of 39.4 kJ/mol is extracted. This value is almost half of that calculated from the open-circuit data of Fig. 3. This phenomenon has been observed in many electrocatalytic studies [23]. Ionic "pumping" causes changes in the work function of the electrode (catalyst) and consequently, in the bonding strength of adsorbed reactants, intermediates and products. This, in turn, results to an increase or decrease of the apparent activation energy of the reaction. In the present study, the observed decrease in the activation energy should be attributed to the weakening of the adsorption strength of the formate species. Thus, the decomposition of the formate, which is considered as the rds, is enhanced.

The effect of H^+ pumping on the rate enhancement ratio, ρ, is shown in Fig. 5a and b. In Fig. 5a, the inlet partial pressures of the reactants were kept constant ($P_{CO} = 1$ kPa and $P_{H_2O} = 2.3$ kPa) and ρ is plotted versus I/2F, the molar flow of H_2. It is clear that H^+ pumping away from the Fe catalyst has a positive effect on the reaction rate. There is a gradual decrease in ρ with temperature; the maximum value of ρ is observed at 823 K, where the electrocatalytic rate, r, becomes 3.2 times the open-circuit rate r_o, i.e. $\rho = 3.2$. Fig. 5b shows the dependence of ρ on I/2F at 873 K and for various CO contents. A weak negative effect of P_{CO} on ρ is observed.

Fig. 6a shows the dependence of the Faradaic efficiency, Λ, on I/2F for a constant inlet composition of $P_{CO} = 1$ kPa and $P_{H_2O} = 2.3$ kPa. In Fig. 6b, the temperature is kept constant at 873 K while P_{CO} varies from 1 to 8.6 kPa. Both Figures show

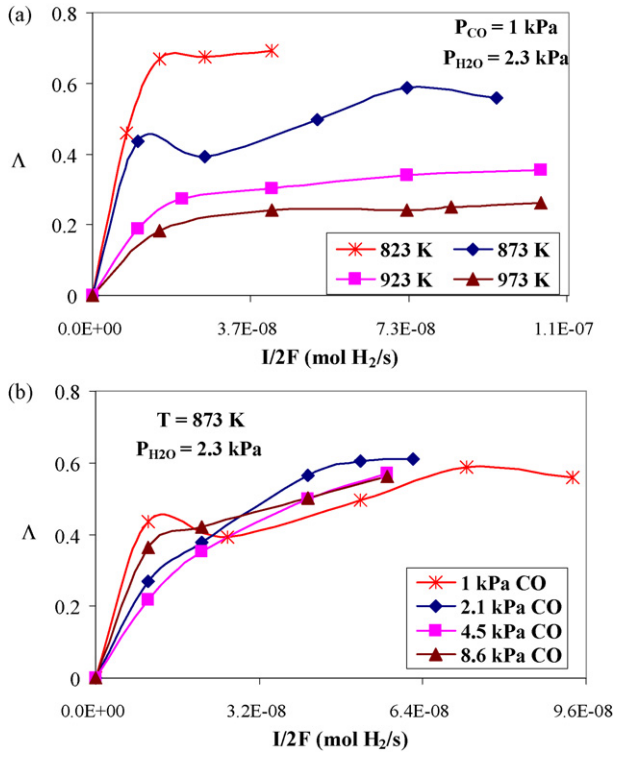

Fig. 6. (a) Dependence of Faradaic efficiency (Λ) on I/2F at various reaction temperatures. P_{CO} = 1 kPa, P_{H_2O} = 2.3 kPa. (b) Dependence of Faradaic efficiency (Λ) on I/2F for various P_{CO}. T = 873 K, P_{H_2O} = 2.3 kPa.

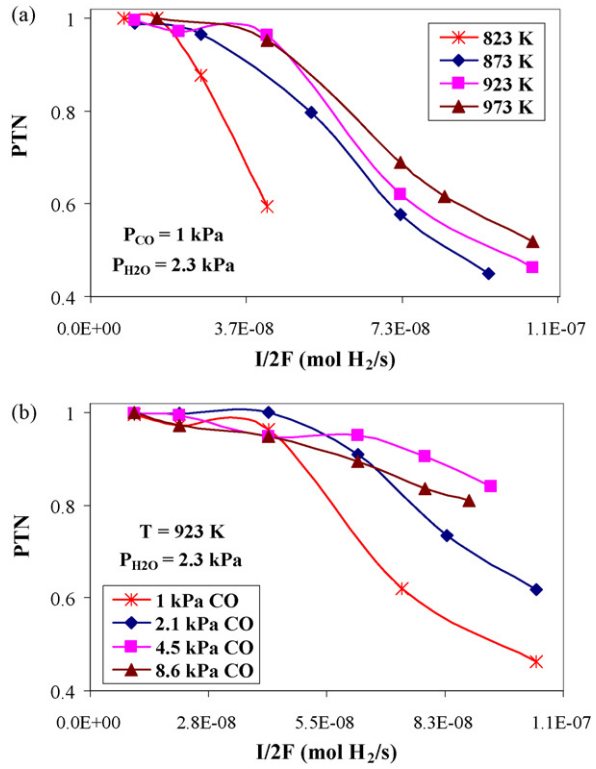

Fig. 7. (a) Dependence of proton transport number (PTN) on I/2F at various reaction temperatures. P_{CO} = 1 kPa, P_{H_2O} = 2.3 kPa. (b) Dependence of proton transport number (PTN) on I/2F for various P_{CO}. T = 923 K, P_{H_2O} = 2.3 kPa.

clearly that Λ does not exceed unity. Therefore, the NEMCA phenomenon is not observed. NEMCA requires $\Lambda > 1.0$. In the present case, H^+ pumping induces a sub-Faradaic effect.

Fig. 7a and b depict the dependence of PTN on I/2F at various temperatures and CO contents, respectively. The PTN values are between 0.45 and 1.0. Fig. 7a shows that at higher temperatures, PTN remains close to unity for a wider range of imposed currents. This is expected, since both hydrogen production and proton conductivity increase with reaction temperature. Fig. 7b shows that for reasonably high P_{CO} values (e.g. $P_{CO} > 4.5$ kPa), PTN numbers higher than 0.8 are maintained. This is not surprising either, because the transport number of the proton conductor is a strong function of both P_{H_2} and P_{CO}. At high P_{CO}, the WGS rate increases and therefore, P_{H_2} increases too.

In order to quantify the role of the WGS reaction in the process of hydrogen production and its subsequent separation from the reaction mixture, a series of experiments in the absence of CO were performed. A H_2O–He mixture (P_{H_2O} = 2.3 kPa) was fed in the reactor and by externally imposing voltages across the cell, hydrogen was produced – via steam electrolysis – and pumped away from the inner chamber (Fig. 1). In Fig. 8a, the current I is presented as a function of the imposed voltage for the temperatures examined. In Fig. 8b, the same dependence is shown but with the WGS reaction taking place, i.e. by introducing CO–H_2O–He mixtures into the inner chamber. It is clear that in the presence of CO, the cell conductivity is significantly improved. Obviously, this is due to the WGS reaction, which constitutes an extra hydrogen source in addition to steam electrolysis.

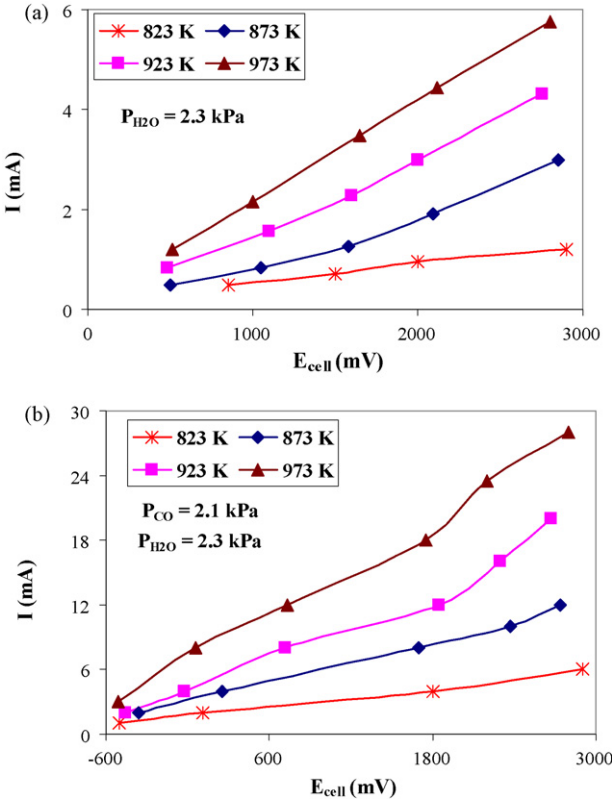

Fig. 8. (a) Dependence of current on cell voltage in the absence of CO. P_{H_2O} = 2.3 kPa. (b) Dependence of current on cell voltage in the presence of CO. P_{CO} = 2.1 kPa, P_{H_2O} = 2.3 kPa.

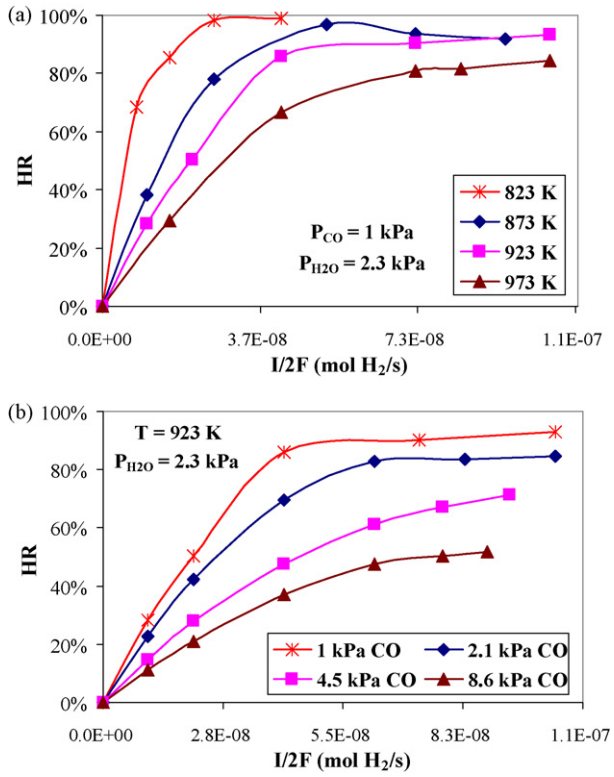

Fig. 9. (a) Dependence of hydrogen removal (HR) on I/2F for various reaction temperatures. P_{CO} = 1 kPa, P_{H_2O} = 2.3 kPa. (b) Dependence of hydrogen removal (HR) on I/2F for various P_{CO}. T = 923 K, P_{H_2O} = 2.3 kPa.

In addition to the transport number, it is very useful to know the fraction of hydrogen produced by the WGS reaction that is electrochemically pumped away from the catalyst. Therefore, a dimensionless number, the 'hydrogen removal (HR) is defined by the following equation:

$$\mathrm{HR} = \frac{\text{rate of } H_2 \text{ pumped to the outer chamber}}{H_2 \text{ produced in the inner chamber}} \times 100 \qquad (12)$$

In Fig. 9a, HR is plotted versus I/2F for constant inlet composition. In Fig. 9b, the reaction temperature is held constant at 923 K and HR is plotted versus I/2F with P_{CO} varying from 1 to 8.6 kPa. In both Figures, HR initially increases with I/2F but at higher currents, it reaches a plateau. Hence, there is an upper current value, above which, electrical energy is offered to the cell without improving the rate of hydrogen pumping.

Fig. 9a and b also show that HR decreases with increasing temperature and P_{CO}, respectively. The effect of temperature can be explained when the WGS reaction rate is compared to the rate of proton transport through the solid electrolyte: the increase in hydrogen production exceeds the increase in proton conductivity of the cell. Note that at T = 823 K and for I/2F > 2.6×10^{-8} mol/s (I = 5 mA), HR is virtually 100% while at T = 973 K the maximum HR values are slightly over 80%. The explanation for the effect of CO (Fig. 9b) is similar: at constant I, the rate of hydrogen removal is constant while hydrogen production increases with increasing P_{CO}. Therefore, HR is higher at low P_{CO}. At P_{CO} = 1 kPa, HR reaches 90% while at P_{CO} = 8.6 kPa, the plateau is slightly above 50%.

The present WGS results can be compared to those obtained previously in a reactor very similar to that of Fig. 1 [25]. In that study, Pd was used as the working electrode (catalyst) and a strontia–zirconia-yttria (SZY) perovskite served as the H^+ conductor. The calculated ρ values were between 1 and 2, i.e. lower than those reported here. On the other hand, a moderate (Λ_{max} = 8) NEMCA effect was observed indicating that as an electrocatalyst, Pd is more active than Fe. Nevertheless, the HR values reported here were significantly higher than those over Pd. In that case, the highest HR was only 20%, attained at T = 873 K.

In a recent study, Matsumoto et al., compared the performance of two proton conductors, SCY and SZY, utilized as hydrogen pumps [30]. In terms of their H^+ "pumping" capacity, SCY was by far superior to SZY. The SCY membrane, however, was not stable because it reacted with CO_2 and therefore its durability and mechanical stability was questionable. In the present experiments there were no signs of degradation. The SCY disk maintained its durability for at least 5 weeks on stream at 823–973 K. It should be pointed out, however, that Matsumoto et al. worked with high CO and CO_2 pressures. In our experiments, the CO and CO_2 contents were kept low; the maximum inlet P_{CO} was about 11.0 kPa (11% of the mixture) and because the reaction conversion was 8–10% at most, the maximum P_{CO_2} in the reactor was of the order of 1.0 kPa. It is worth investigating the stability of the reactor at much higher CO and CO_2 contents. Work in this direction is currently in progress.

4. Conclusions

The WGS reaction was studied in an HTPC reactor. A kinetic model of the form $r = kP_{CO}^{a}$ was found to fit both catalytic and electrocatalytic measurements in a satisfactory manner. The calculated activation energy for the intrinsic catalytic reaction was 77.4 kJ/mol while under closed circuit, an up to 50% decrease in the activation energy was observed. The electrochemical promotion parameters 'ρ' and 'Λ', attained relatively low values. The maximum ρ was about 3.2. All the Λ values remained below unity, indicating a sub-Faradaic process. In terms of hydrogen removal and separation, very encouraging results were obtained: the hydrogen pumping efficiency, expressed in HR values, could be as high as 90–100%, indicating that almost all hydrogen produced by the WGS reaction could be pumped away from the reaction mixture. Additionally, the present system is advantageous for practical applications because both hydrogen formation is electochemically enhanced and simultaneously separated from the reaction mixture.

Acknowledgements

We gratefully acknowledge support by the European Union, the General Secretariat of Research & Technology and the Hellenic Petroleum Co. under the PENED 2003 Programme.

We also thank Dr. Lipilin (Ekaterinenburg, Russia) for the preparation of the glass material that sealed the ceramic tube to the H^+ disk.

References

[1] Y. Sato, K. Terada, Y. Soma, T. Miyao, S. Naito, Catal. Commun. 7 (2005) 91.
[2] P. Panayiotopoulou, D.I. Kondarides, J. Catal. 225 (2004) 327.
[3] Y. Sato, K. Terada, S. Hasegawa, T. Miyao, S. Naito, Appl. Catal. A 296 (2005) 80.
[4] D.C. Grenoble, M.M. Estadt, D.F. Ollis, J. Catal. 67 (1981) 90.
[5] R.J. Gorte, S. Zhao, Catal. Today 104 (2005) 18.
[6] T. Bunluesin, R.J. Gorte, G.W. Graham, Appl. Catal. B 15 (2005) 107.
[7] C. Wheeler, A. Jhalani, E.J. Klein, S. Tummala, L.D. Schmidt, J. Catal. 223 (2004) 191.
[8] E.S. Bickford, S. Velu, C. Song, Catal. Today 99 (2005) 347.
[9] D.G. Rethwisch, J.A. Dumesic, J. Catal. 101 (1986) 35.
[10] G.C. Chinchen, R.H. Logan, M.S. Spencer, Appl. Catal. 12 (1984) 97.
[11] T. Salmi, L.E. Lindfors, S. Bostrom, Chem. Eng. Sci. 41 (1986) 929.
[12] C. Rhodes, G.J. Hutchings, A.M. Ward, Catal. Today 23 (1995) 43.
[13] R.L. Keiski, T. Salmi, P. Niemisto, J. Ainassari, V.J. Pohjola, Appl. Catal. A 137 (1996) 349.
[14] Y. Lei, N.W. Cant, D.L. Trimm, Chem. Eng. J. 114 (2005) 81.
[15] B.-T. Teng, J. Chang, J. Yang, G. Wang, C.-H. Zhang, Y.-Y. Xu, H.-W. Xiang, Y.-W. Li, Fuel 84 (2005) 917.
[16] S. Hilaire, X. Wang, T. Luo, R.J. Gorte, J. Wagner, Appl. Catal. A 258 (2004) 271.
[17] G. Jacobs, E. Chenu, P.M. Patterson, L. Williams, D. Sparks, G. Thomas, B.H. Davis, Appl. Catal. A 258 (2004) 203.
[18] A. Basile, G. Chiappetta, S. Tosti, V. Violante, Sep. Purif. Technol. 25 (2001) 549.
[19] S. Tosti, L. Bettinali, V. Violante, Int. J. Hydrogen Energy 25 (2000) 319.
[20] S. Tosti, L. Bettinali, V. Violante, Ind. Eng. Chem. Res. 30 (1991) 585.
[21] M. Stoukides, Cat.Rev.-Sci. Eng. 41 (2000) 1.
[22] H. Iwahara, Y. Asakura, K. Katahira, M. Tanaka, Solid State Ionics 168 (2004) 299.
[23] C.G. Vayenas, S. Bebelis, C. Pliangos, S. Brosda, D. Tsiplakides, Electrochemical Activation of Catalysis, Kluwer Academic/Plenum, New York, 2001.
[24] C.G. Vayenas, M.M. Jaksic, S. Bebelis, S.G. Neophytides, The electrochemical activation of catalytic reactions, in: J.O.M. Bockris, B.E. Conway, W.R.E. White (Eds.), Modern Aspects in Electrochemistry, 29, Plenum, 1996, p. 57.
[25] C. Kokkofitis, M. Ouzounidou, A. Skodra, M. Stoukides, Solid State Ionics 178 (2007) 475.
[26] G. Karagiannakis, C. Kokkofitis, S. Zisekas, M. Stoukides, Catal. Today 104 (2005) 219.
[27] C. Kokkofitis, G. Karagiannakis, S. Zisekas, M. Stoukides, J. Catal. 234 (2005) 476.
[28] H. Iwahara, T. Yajima, T. Hibino, K. Ozaki, H. Suzuki, Solid State Ionics 61 (1993) 65.
[29] S. Zhao, R.J. Gorte, Catal. Lett. 92 (2004) 75.
[30] H. Matsumoto, M. Okubo, S. Hamajima, K. Katahira, H. Iwahara, Solid State Ionics 152 (2002) 715.